www.czasopisma.pan.pl PAN www.journals.pan.pl

jet INTL JOURNAL OF ELECTRONICS AND TELECOMMUNICATIONS, 2021, VOL. 67, NO. 3, PP. 431-436
Manuscript received April 26, 2020; revised July, 2021 DOI: 10.24425/ijet.2021.137830

Ergodic Channel Capacity of PPM-Coded Optical MIMO Communications Under Combined Effects

Minghua Cao, Yue Zhang, Zhongjiang Kang, and Huiqin Wang

***Abstract*—The ergodic channel capacity of wireless optical multiple-input multiple-output (MIMO) system with pulse position modulation (PPM) is investigated. The combined effects of atmospheric turbulence, atmospheric attenuation, pointing error and channel spatial correlation are taken into consideration. The expression of ergodic channel capacity is derived, and is further performed by Wilkinson approximation method for simplicity. The simulation results indicated that the strong spatial correlation has the greatest influence on the ergodic channel capacity, followed by pointing errors and atmospheric turbulence. Moreover, the ergodic channel capacity growth brought by space diversity only performs well under independent and weakly correlated channels. Properly increasing the size and spacing of the receiving apertures is an effective means of effectively increasing the ergodic channel capacity.**

***Keywords*—atmospheric channel, ergodic channel capacity, pulse position modulation, spatial correlation, optical wireless communication**

I. Introduction

OPTICAL wireless communication (OWC) has been widely concerned by researchers in recent years due to its security, high transmission rate and wide spectrum range [1]. However, the OWC link performance heavily dependent on the characteristics of atmospheric channel [2]. Given that MIMO technology can effectively resist the atmospheric turbulence effect and promote the channel capacity without additional spectrum resources [3-4]. Therefore, it has become a promising technology suited for OWC. So far, a number of researches have been developed for the OWC MIMO systems. For example, the ergodic channel capacity of OWC MIMO systems with On-Off Key (OOK) over log-normal turbulence channel is analyzed in [5]. The ergodic channel capacity of OWC MIMO systems with Multiple-Pulse Position Modulation (MPPM) over gamma-gamma turbulence channel is analyzed in [6]. The ergodic channel capacity and outage probability of OWC MIMO system with OOK under effects of atmospheric turbulence and atmospheric attenuation over gamma-gamma turbulence channel is analyzed in [7]. The adaptive multivariate precomputed B-spline and Barycentric Lagrange interpolation-based lookup table (B^2LUT) statistical model for MIMO OWC system ergodic channel capacity estimation under generalized Málaga (M)-distributed atmospheric turbulence channel is analyzed in [8].

In addition to atmospheric turbulence channel, there are many other influencing factors like pointing error and spatial correlation present in the practical OWC MIMO systems. The effects of spatial correlation on BER and outage capacity are discussed in [9-12]. The influence of pointing error on BER and outage probability are studied in [13-15]. Furthermore, the BER performance of OWC MIMO system with differential phase shift keying (DPSK) is discussed in [16] by considering the effects of atmospheric turbulence and pointing error.

However, the ergodic channel capacity of OWC MIMO system is influenced by all the aforementioned factors. It is particularly important to study the OWC MIMO system performance when multiple influencing factors coexist. Therefore, we discuss the ergodic channel capacity under the combined effects of atmospheric turbulence, atmospheric attenuation, pointing error and channel spatial correlation in the following sections.

The rest of this paper is organized as follows: In Section 2, the correlated channel model is introduced. In Section 3, the ergodic channel capacity with combined effects is analyzed, and its approximate expression is derived for simplicity. Numerical simulation results are given in Section 4. Finally, a conclusion is given in Section 5.

II. System Model

For a OWC MIMO system, as shown in Fig. 1, M and N denote the number of laser diodes (LDs) and photodetectors (PDs), respectively. Assuming the total transmitting power is E_s, therefore, the average power of each laser is E_s/M. When using Q-ary PPM modulation format, every symbol contains $\log_2 Q$ bits information. If a symbol period is T_s, then the time slot is $T = T_s/Q$.

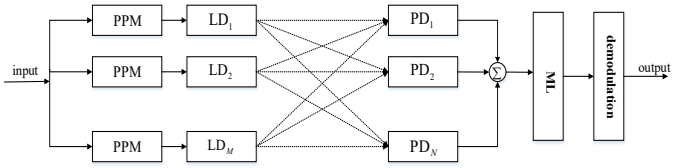

Fig. 1. Block scheme of the OWC MIMO system.

This work was supported in part by the National Natural Science Foundation of China under Grant 61861026 and 61875080.

Minghua Cao, Yue Zhang, Zhongjiang Kang and Huiqin Wang are with School of Computer and Communication, Lanzhou University of Technology, Lanzhou, China, (e-mail: caominghua@lut.edu.cn, zyue940209@163.com, txgckzj@163.com, 15117024169@139.com).

When considering combined effects, the signal received by the n-th photodetector, denoted as $y^{(n)}$, can be described as

$$y^{(n)} = \frac{n_s}{M}\sum_{m=1}^{M} x^{(m)} g_{nm} + n_b n_0 \tag{1}$$

where $n_s = \eta E_s / \varepsilon f$ denotes the average number of photoelectrons counted in a pulse at one PD over nonfading channel, η denotes the photoelectric conversion efficiency, ε denotes the Planck constant, f denotes the optical carrier frequency, $x^{(m)}$ denotes the signal sent by the m-th laser, n_0 denotes the noise vector, $n_b = \eta E_b / \varepsilon f$ denotes the average count rate of background noise, E_b denotes the average noise power of detectors, g_{nm} denotes the sub-channel correlation caused light intensity attenuation coefficient by the m-th laser and the n-th photodetector.

Assuming $H = (h_{nm})_{NM}$ as the light intensity attenuation coefficient matrix under the combined effects when the sub-channels are independent. Therefore, the light intensity attenuation coefficient matrix G of correlated fading channel under combined effects can be written as

$$\boldsymbol{G} = \boldsymbol{R}_r \cdot \boldsymbol{H} \cdot \boldsymbol{R}_t = [\boldsymbol{g_{nm}}]_{NM} \tag{2}$$

where $\boldsymbol{R}_r$ is the $N \times N$ receiver correlation matrix, and $\boldsymbol{R}_t$ is the $M \times M$ transmitter correlation matrix [17]. The $\boldsymbol{R}_r$ and $\boldsymbol{R}_t$ can be written as

$$\boldsymbol{R}_t = \begin{pmatrix} 1 & r_t & r_t^2 & \cdots & r_t^{M-1} \\ r_t & 1 & r_t & \cdots & r_t^{M-2} \\ \vdots & \vdots & \vdots & \ddots & \vdots \\ r_t^{M-1} & r_t^{M-2} & r_t^{M-3} & \cdots & 1 \end{pmatrix} \tag{3}$$

and

$$\boldsymbol{R}_r = \begin{pmatrix} 1 & r_r & r_r^2 & \cdots & r_r^{N-1} \\ r_r & 1 & r_r & \cdots & r_r^{N-2} \\ \vdots & \vdots & \vdots & \ddots & \vdots \\ r_r^{N-1} & r_r^{N-2} & r_r^{N-3} & \cdots & 1 \end{pmatrix} \tag{4}$$

where $|r_t| < 1, |r_r| < 1$.

It should be noted that h_{nm} can be written as

$$h_{nm} = h_{nm}^{l} \cdot h_{nm}^{a} \cdot h_{nm}^{p} = A_0 e^{X_{nm} - 2R_{nm}^2/\omega^2 - \sigma L} \tag{5}$$

where $h_{nm}^{l} = \exp(-\sigma L)$ denotes the atmospheric attenuation caused by path loss over a distance of L, σ denotes the attenuation coefficient. Generally, the atmospheric attenuation can be expressed as a constant when the transmission distance is determined. $h_{nm}^{a} = \exp(X_{nm})$ denotes the random attenuation of light intensity caused by weak turbulence and usually follows lognormal distribution [18]. X_{nm} is a normally distributed variable with mean $\mu_{X_{nm}} = -1/2\,\sigma_{X_{nm}}^2$ and variance $\sigma_{X_{nm}}^2 = 1.23 C_n^2 k^{7/6} L^{11/6}$. C_n^2 is the structure constant of atmospheric refractive index, k is the wave number. $h_{nm}^{p} \approx A_0 \exp(-2R_{nm}^2/\omega^2)$ denotes the random attenuation of light intensity caused by pointing error. $A_0 = [\mathrm{erf}(v)]^2$ is the fraction of the collected power at R_{nm}=0, R_{nm} is the radial displacement from the m-th transmitting beam center to the n-th receiving aperture center, $\omega^2 = \omega_L^2 \sqrt{\pi}\,\mathrm{erf}(v) / [2v \exp(-v^2)]$ is the equivalent beam width, $v = \sqrt{\pi} a / (\sqrt{2}\omega_L)$ is the ratio of a to ω_L, ω_L is the waist of the receiving beam, a is the radius of the receiving aperture.

Therefore, the intensity attenuation coefficient under the combined effects can be written as

$$g_{nm} = \left(r_r^{|i-j|}\right)_{i,j=1,2K\,N} \cdot \left[A_0 \exp\left(X_{nm} - 2R_{nm}^2/\omega^2 - \sigma L\right)\right] \cdot \left(r_t^{|i-j|}\right)_{i,j=1,2K\,M} \tag{6}$$

III. Ergodic Channel Capacity Under Combined Effects

The channel capacity of optical MIMO system can be described as

$$C = \max_{p(x)} I(x;y) \tag{7}$$

where $p(x)$ is the probability density function (PDF) of vector x. The mutual information $I(x;y)$ can be defined by

$$I(x;y) = H(y) - H(y \mid x) \tag{8}$$

where $H(y)$ denotes the entropy of vector y. $H(y \mid x)$ denotes the conditional entropy. The instantaneous channel capacity of optical MIMO system can be given by

$$C = \log_2 Q \cdot \left[1 - \exp\left(-\frac{\eta E_s \sum_{m=1}^{M}\sum_{n=1}^{N} g_{nm}}{\varepsilon f M}\right)\right] \tag{9}$$

Equation (9) indicates that the instantaneous channel capacity is a random variable on fading channel. Therefore, the ergodic channel capacity of the PPM-coded optical MIMO system can be written as

$$\begin{aligned} C_{avg} &= E[C] \\ &= \int_0^\infty \int_0^\infty \cdots \int_0^\infty f(g_{nm}) \log_2 Q \left[1 - \exp\left(-\frac{\eta E_s \sum_{m=1}^{M}\sum_{n=1}^{N} g_{nm}}{\varepsilon f M}\right)\right] \mathrm{d}g_{11} \ldots \mathrm{d}g_{NM} \end{aligned} \tag{10}$$

Suppose $S = \sum_{m=1}^{M}\sum_{n=1}^{N} g_{nm}$, then

$$\begin{aligned} S &= \sum_{m=1}^{M}\sum_{n=1}^{N} g_{nm} \\ &= \sum_{m=1}^{M}\sum_{n=1}^{N} \left(r_r^{|i-j|}\right)_{i,j=1,2\ldots N} \cdot \left[A_0 \exp\left(X_{nm} - 2R_{nm}^2/\omega^2 - \sigma L\right)\right] \cdot \left(r_t^{|i-j|}\right)_{i,j=1,2\ldots M} \\ &= \exp\left(-2R^2/\omega^2\right) \cdot \exp(-\sigma L) \cdot \sum_{m=1}^{M}\sum_{n=1}^{N} \left(r_r^{|i-j|}\right)_{i,j=1,2\ldots N} \\ &\quad \cdot \left[A_0 \exp\left(X_{nm} - 2(R_{nm}^2 - R^2)/\omega^2\right)\right] \cdot \left(r_t^{|i-j|}\right)_{i,j=1,2\ldots M} \\ &= A_0 l_0 \exp(-\delta) \cdot \sum_{m=1}^{M}\sum_{n=1}^{N} \left(r_r^{|i-j|}\right)_{i,j=1,2\ldots N} \cdot \exp(B_{nm}) \cdot \left(r_t^{|i-j|}\right)_{i,j=1,2\ldots M} \end{aligned} \tag{11}$$

where $l_0 = \exp(-\sigma L)$ denotes atmospheric attenuation, $B_{nm} = X_{nm} - 2(R_{nm}^2 - R^2)/\omega^2$, $\delta = \frac{2R^2}{\omega^2}$, and $f_\delta(\delta) = \gamma^2 e^{-\gamma^2\delta}$ is the PDF of δ. $\gamma = \omega/(2\sigma_s)$ denotes the ratio of ω to σ_s, where σ_s is the standard deviation of jitter. And σ_s^2 is generally used to denote the deviation of pointing error.

For independent channels, B_{nm} follows the normal distribution. Its mean $\mu_{B_{nm}}$ and variance $\sigma_{B_{nm}}^2$ can be written as

$$\begin{cases} \mu_{B_{nm}} = \mu_{X_{nm}} - \frac{2}{\omega^2}\|\boldsymbol{P_m} - \boldsymbol{P_n}\|^2 \\ \sigma_{B_{nm}}^2 = \sigma_{X_{nm}}^2 + \frac{16\sigma_s^2}{\omega^4}(\boldsymbol{P_m} - \boldsymbol{P_n})^T(\boldsymbol{P_m} - \boldsymbol{P_n}) \end{cases} \tag{12}$$

where $\sigma_{X_{nm}}^2$ denotes the turbulence intensity, $\boldsymbol{P}_i$ ($\boldsymbol{P}_i \in \Im$, $\Im$ is a set of coordinates which includes all receiving apertures) denotes the coordinate vector to the center of the i-th receiving aperture, and $\boldsymbol{O}_j$ is the coordinate vector to the center of the j-th transmitting beam footprint at the receiver side. Therefore,

$$\begin{cases} \boldsymbol{O_m} = \begin{bmatrix} \boldsymbol{X'} \\ \boldsymbol{Y'} \end{bmatrix} + \boldsymbol{P_m} \\ R_{nm}^2 = \|\boldsymbol{O_m} - \boldsymbol{P_n}\|^2 = \left\| \begin{bmatrix} \boldsymbol{X'} \\ \boldsymbol{Y'} \end{bmatrix} + \boldsymbol{P_m} - \boldsymbol{P_n} \right\|^2 \end{cases} \tag{13}$$

where $\boldsymbol{X'}, \boldsymbol{Y'} \sim N(0, \sigma_s^2)$, $\boldsymbol{X'}$ and $\boldsymbol{Y'}$ are random displacement vectors in the x-direction and y-direction, respectively.

When B_{nm} multiplies the correlation matrix $\boldsymbol{R}_t$ and $\boldsymbol{R}_r$, the result still going to follow the normal distribution. It can be written as

$$\sum_{k=1}^{NM} \exp(V_k) = \sum_{m=1}^{M}\sum_{n=1}^{N} \left(r_r^{|i-j|}\right)_{i,j=1,2\ldots N} \cdot \exp(B_{nm}) \cdot \left(r_t^{|i-j|}\right)_{i,j=1,2\ldots M} \tag{14}$$

where V_k follows the normal distribution. Its mean and variance can be expressed as

$$\begin{cases} \mu_{V_k} = \mu_{B_{nm}} \cdot \left(\frac{1-r_t^M}{1-r_t}\right) \cdot \left(\frac{1-r_r^N}{1-r_r}\right) \\ \sigma_{V_k}^2 = \sigma_{B_{nm}}^2 \cdot \left(\frac{1-r_t^{2M}}{1-r_t^2}\right) \cdot \left(\frac{1-r_r^{2N}}{1-r_r^2}\right) \end{cases} \tag{15}$$

According to Wilkinson method [19], the sum of lognormal variables can be approximately express by another lognormal variable. In other words, there is an approximation as $\exp(W) \approx \sum_{k=1}^{NM} \exp(V_k)$, where W follows normal distribution, its mean and variance is

$$\begin{cases} \mu_W = 2\ln\alpha - \frac{1}{2}\ln\beta \\ \sigma_W^2 = \ln\beta - 2\ln\alpha \end{cases} \tag{16}$$

where α and β can be written as

$$\alpha = \sum_{k=1}^{MN} e^{\mu_{V_k} + \sigma_{V_k}^2/2} \tag{17}$$

and

$$\begin{aligned} \beta = &\sum_{k=1}^{NM} \exp(2\mu_{V_k} + 2\sigma_{V_k}^2) \\ &+ 2\sum_{k=1}^{NM-1}\sum_{j=k+1}^{NM} \left\{ \exp(\mu_{V_k} + \mu_{V_j}) \cdot \exp\left[\frac{1}{2}(\sigma_{V_k}^2 + \sigma_{V_j}^2 + 2r_{kj}\sigma_{V_k}\sigma_{V_j})\right] \right\} \end{aligned} \tag{18}$$

As a result, (11) can be simplified as

$$S = A_0 l_0 \exp(W - \delta) = A_0 l_0 \exp(U) \tag{19}$$

where $U = W - \delta$. The PDF of U can then be expressed as

$$f_U(U) = \int_0^\infty f_{U|\delta}(U \mid \delta) f_\delta(\delta)\, d\delta \tag{20}$$

where

$$f_{U|\delta}(U|\delta) = \frac{1}{\sqrt{2\pi}\sigma_W} \exp\left\{ -\frac{[U - (\mu_W - \delta)]^2}{2\sigma_W^2} \right\} \tag{21}$$

Substituting $f_\delta(\delta)$ and (21) into (20), the result can be written as

$$f_U(U) = \frac{\gamma^2}{2} \exp\left(\frac{\gamma^4\sigma_W^2}{2} - \gamma^2\mu_W\right) \exp(\gamma^2 U) \cdot \operatorname{erfc}\left(\frac{U + \gamma^2\sigma_W^2 - \mu_W}{\sqrt{2}\sigma_W}\right) \tag{22}$$

As a result, the PDF of $S = A_0 l_0 \exp(U)$ can be expressed as

$$\begin{aligned} f_S(S) = \frac{1}{S} f_U(\ln S) = &\frac{\gamma^2}{2S} \exp\left(\frac{\gamma^4\sigma_W^2}{2} - \gamma^2\mu_W\right) \exp(\gamma^2 \ln S) \\ &\cdot \operatorname{erfc}\left(\frac{\ln S + \gamma^2\sigma_W^2 - \mu_W}{\sqrt{2}\sigma_W}\right) \end{aligned} \tag{23}$$

Subsequently, substituting (19) and (23) into (10), the ergodic channel capacity of the OWC MIMO system under combined effects can then be expressed as

$$\begin{aligned} C_{avg} = \log_2 Q - \log_2 Q \cdot &\int_0^\infty \frac{\gamma^2}{2S} \exp\left(\frac{\gamma^4\sigma_W^2}{2} - \gamma^2\mu_W\right) \exp(\gamma^2 \ln S) \\ &\cdot \operatorname{erfc}\left(\frac{\ln S + \gamma^2\sigma_W^2 - \mu_W}{\sqrt{2}\sigma_W}\right) \exp\left(-\frac{\eta E_s S}{\varepsilon f M}\right) \mathrm{dS} \end{aligned} \tag{24}$$

It is evident from (24) that the ergodic channel capacity is related to parameters Q, η, E_s, M and S. It should be noted that S is affected by parameters l_0, $\sigma_{\chi_{nm}}^2$, σ_s^2, a and r_r, r_t.

In this section, the ergodic channel capacity of 2×2 and 4×4 OWC MIMO system with combined effects have been numerically investigated based on the foregoing analysis. And the curves of ergodic channel capacity are based on the proposed approximate equations. The simulation parameters are set as follows: $\eta = 0.5$, $Q = 8$, $\lambda = 1550$ nm, $L = 1000$ m, $C_n^2 = 2.23\times10^{-14}$ $\mathrm{m}^{-2/3}$, $h_{nm}^1 = l_0 = 0.9$, $\sigma_s^2 = 0.1$ and $\sigma_{X_{nm}}^2 = 0.4$.

Figure 2 shows the ergodic channel capacity (C_{avg}) of a 4×4 OWC MIMO system with different channel correlation coefficient, where iid denotes independent and identical distributed channel, corr denotes correlated channel, appro. denotes the simplified approximation of (24), exact denotes the

theoretical value of (10), CE($\sigma_{X_{nm}}^2 = 0.4$, $\sigma_s^2 = 0.1$, $l_0 = 0.9$) denotes the channel under combined effects.

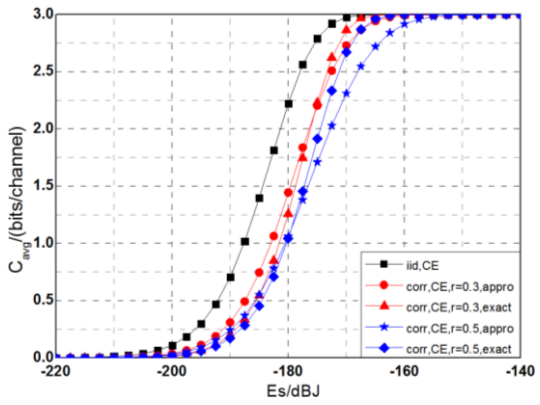

Fig. 2. Theoretical and approximated values of ergodic channel capacity for a 4×4 OWC MIMO system under combined effects

It is evident from Fig. 2 that the performance of our approximation are slightly worse than the corresponding exact one. For example, when the correlation coefficient is 0.3, the curves of approximation and theoretical values reach to their maximum separation value of 0.218 bit/channel at E_s =-182.5 dBJ. Similarly, when the correlation coefficient is 0.5, the curves reach to their maximum separation value of 0.317 bit/channel at E_s =-170 dBJ. Note that the computation complexity of our approximation is much lower than the theoretical one, which is reduced from a $M\times N$ fold integrals to a single integral. Therefore, the performance degradation caused by simplification is worthwhile.

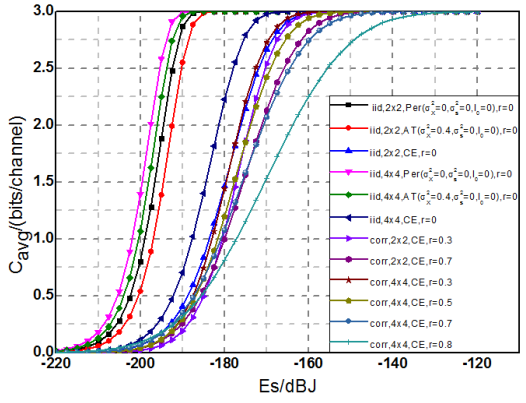

Fig. 3. The ergodic channel capacity under different conditions

Figure 3 shows the curves of C_{avg} versus E_s with different conditions. As can be concluded from Fig. 3 that the C_{avg} increase with the increasing E_s . Especially, when E_s surpasses a threshold, the ergodic channel capacity reaches saturation. Moreover, the CE will seriously impact on the ergodic channel capacity. For example, when $E_s = -190$ dBJ, the ergodic channel capacity reduced by 2.24 bits/channel compared with the Per case in 4×4 system. It should be noted that the influence of pointing error is more significant than atmospheric attenuation and atmospheric turbulence. Furthermore, the C_{avg} decrease with the increasing correlation coefficient under the combined effects. When the correlation coefficient is 0, 0.3, 0.5, 0.7 and 0.8, the threshold values of capacity saturation are - 166 dBJ, - 160 dBJ, - 153 dBJ, -144 dBJ and - 130 dBJ, respectively. Compared with the ideal transmission condition (Per), the presence of CE seriously impact on the ergodic channel capacity. For example, when E_s =-190 dBJ, the ergodic channel capacity decreased by about 2.6 bit/channel and the capacity saturation threshold increased by about 25 dBJ of a 4×4 OWC MIMO system under combined effects compared with the ideal transmission condition. In addition, when the ergodic channel capacity reaches its saturation, the power loss caused by the combined effects is 15 dBJ in 4×4 system. While the power loss caused by the strong correlation is 22.5 dBJ, which is greater than that of combined effects. Therefore, it can be considered that strong correlation has more effect on ergodic channel capacity than combined effects.

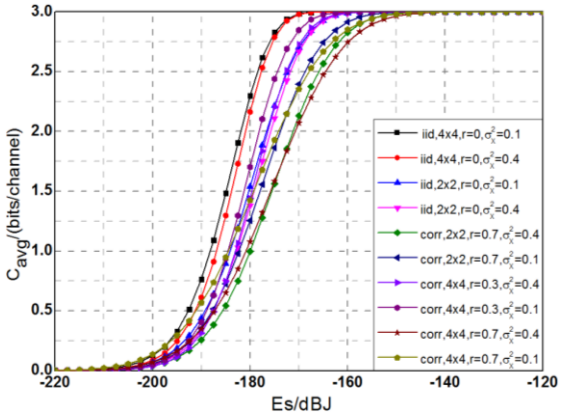

Fig. 4. The relationship of ergodic channel capacity with different correlation coefficients and turbulence intensity

Figure 4 describes the relationship of C_{avg} versus E_s with different correlation coefficients and turbulence intensity. All C_{avg} curves are performed under the condition of CE. It is evident from this figure that the ergodic channel capacity decrease with the increasing turbulence intensity and correlation coefficient. Moreover, the effect of turbulence intensity on the ergodic channel capacity increases with the increasing channel correlation. For example, in a 4×4 OWC MIMO system when E_s=-170 dBJ and $\sigma_{X_{nm}}^2 = 0.4$, the ergodic channel capacity decreased by 0.05 bit/channel, 0.2 bit/channel and 0.35 bit/channel compared with that at $\sigma_{X_{nm}}^2 = 0.1$ when the correlation coefficients are 0, 0.3 and 0.7, respectively. Moreover, the capacity saturation threshold increased by about 0.8 dBJ, 1.5 dBJ and 2.6 dBJ, respectively. Furthermore, when the channel is independent or weakly correlated, the benefits achieved by spatial diversity is dominated in a OWC MIMO system under combined effects. Otherwise, the benefits achieved by spatial diversity is not sufficient to compensate for the performance degradation caused by atmospheric turbulence and strong channel correlation.

Figure 5 shows the curves of C_{avg} versus E_s with different correlation coefficients and jitter variances. All C_{avg} curves are performed under the condition of CE. It is evident from this figure that the ergodic channel capacity decreases significantly with the increasing jitter variance and channel correlation. For example, in a 4×4 OWC MIMO system when E_s =-170 dBJ and $\sigma_s^2 = 0.3$, the ergodic channel capacity decreased by 0.18 bit/channel, 0.45 bit/channel and 0.7 bit/channel compared with that of $\sigma_s^2 = 0.1$ when the correlation coefficient are 0, 0.3, 0.8 respectively. The capacity saturation threshold increased by about 3 dBJ, 5 dBJ and 8 dBJ, respectively. Similar to the results of Fig. 4, the benefits achieved by spatial diversity is remarkable under independent and weak correlated channel.

Therefore, the ergodic channel capacity decreases with the increasing of $\sigma_{X_{nm}}^2$ and σ_s^2 . And the increase of σ_s^2 has a greater impact on the ergodic channel capacity of the OWC MIMO system than $\sigma_{X_{nm}}^2$.

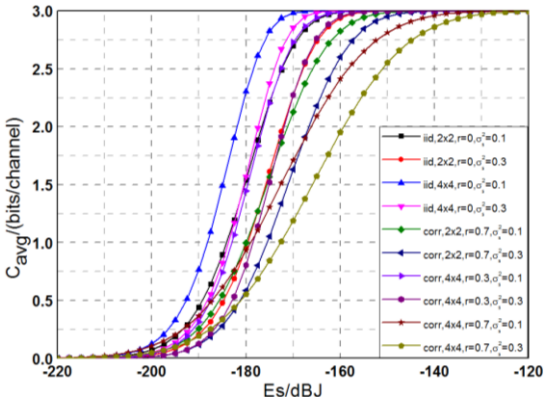

Fig. 5. The relationship of ergodic channel capacity with correlation coefficients and jitter variance

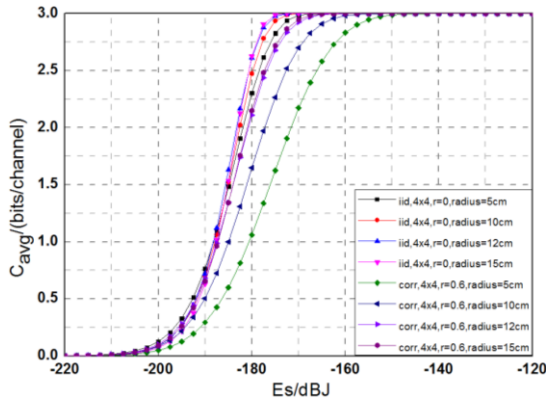

Fig. 6. The relationship of ergodic channel capacity and receiving aperture sizes under combined effects

Figure 6 shows the curves of C_{avg} versus E_s of different receiving aperture sizes under combined effects. It is evident that the ergodic channel capacity increase obviously with the increasing receiving aperture radius when the channel is correlated. For example, when $E_s = -180$ dBJ, compared to 5 cm radius, the ergodic channel capacity with receiving aperture radius of 10 cm, 12 cm, and 15 cm are increased by 0.65 bit/channel, 0.48 bit/channel, and 0.48 bit/channel, respectively. When the channel is independent, the channel capacity is only increased by 0.22 bit/channel, 0.13 bit/channel, and 0.13 bit/channel, respectively. However, the increase of ergodic channel capacity will stop when the aperture size increased to a certain level. As a result, appropriately increasing receiving aperture size can increase the ergodic channel capacity, but unrestricted increase has no obvious effect on resisting combined effects.

CONCLUSION

The ergodic channel capacity of OWC MIMO system over correlated fading channel under combined effects is studied. The approximate expression of the ergodic channel capacity for PPM modulation is derived to reduce the computational complexity. The results indicate that: 1) Strong spatial channel correlation has the most seriously impact on the ergodic channel capacity, followed by pointing error and atmospheric turbulence. 2) The ergodic channel capacity improvement bring by spatial diversity can only be achieved under independent and weak turbulence channel. Therefore, all promoting factors should be considered comprehensively to maximize the ergodic channel capacity of an OWC MIMO system.

REFERENCES

[1] N. Joshi and P. K. Sharma, "Performance of wireless optical communication in S-distributed turbulence," IEEE Photonic Technology Letters, vol. 28, no. 2, pp. 151-154, Oct. 2016. DOI: 10.1109/LPT.2015.2487605

[2] J. Anshul, and M. R. Bhatnagar, "Free-space optical communication: a diversity-multiplexing trade-off perspective," IEEE Transactions on Information Theory, vol. 65, no. 2, pp. 1113-1125, 2019. DOI: 10.1109/TIT.2018.2856116.

[3] P. Kaur, V. K. Jain, and S. Kar, "Performance analysis of free space optical links using multi-input multi-output and aperture averaging in presence of turbulence and various weather conditions," Communications Iet, vol. 9, no. 8, pp. 1104-1109, May. 2015. DOI: 10.1049/iet-com.2014.0926

[4] Y. Zhang, H. Yu, J. Zhang, and Y. Zhu, "Space codes for MIMO optical wireless communications: Error performance criterion and code construction," *IEEE Transcation on Wireless Communication*, vol. 16, no. 5, pp. 3072-3085, 2017. DOI: 10.1109/TWC.2017.2675398

[5] D. A. Luong, T. C. Thang, and A. T. Pham, "Average capacity of MIMO/FSO systems with equal gain combining over log-normal channels," International Conference on Ubiquitous & Future Networks. IEEE, pp. 306-309, Jul. 2013. DOI: 10.1109/ICUFN.2013.6614831

[6] H. S. Khallaf, and H. M. H. Shalaby, "Closed form expressions for SER and capacity of shot noise limited MIMO-FSO system adopting MPPM over gamma-gamma atmospheric turbulence channels," *IEEE Photonics Conference*, CA, USA, Oct. 2014, pp. 619-620. DOI: 10.1109/IPCon.2014.6995292

[7] L. Han and Y. You, "Performance of multiple input multiple output free space optical communication under atmospheric turbulence and atmospheric attenuation," *Chinese Journal of Lasers*, vol. 43, no. 7, pp. 0706004, July 2016. DOI: 10.3788/CJL201643.0706004

[8] I. A. Alimi, A. M. Abdalla, J. Rodriguez, P. P. Monteiro, and A. L. Teixeira, "Spatial interpolated lookup tables (LUTs) models for ergodic capacity of MIMO FSO systems," *IEEE Photonics Technology Letters*, vol. 29, no. 7, pp. 583-586, Apr. 2017. DOI: 10.1109/LPT.2017.2669337

[9] G. Yang, M. A. Khalighi, Z. Gassemlooy, and S. Bourennane, "Performance analysis of space-diversity free-space optical systems over the correlated Gamma-Gamma fading channel using Padé approximation method," *IET Communications*, vol. 8, no. 13, pp. 2246-2255, Sept. 2014. DOI: 10.1049/iet-com.2013.0962

[10] H. S. Khallaf, J. M. Garrido-Balsells, H. M. H. Shalaby, and Seiichi Sampei, "SER analysis of MPPM-Coded MIMO-FSO system over uncorrelated and correlated Gamma-Gamma atmospheric turbulence channels," *Optics Communications*, vol. 356, pp. 530-535, Aug. 2015. DOI: 10.1016/j.optcom.2015.08.060

[11] M. Petkovic, J. Anastasov, G.T. Djordjevic, and P. Ivanis, "Impact of correlation on outage performance of FSO system with switch-and-stay diversity receiver," *2015 IEEE International Conference on Communications (ICC)*, London, 2015, pp. 2756–2761, DOI: 10.1109/ICC.2015.7248743.

[12] T. Ozbilgin, and M. Koca, "Inter-aperture correlation in MIMO free space optical systems," *Optics Communications,* vol. 353, pp. 139–146, May. 2015. DOI: 10.1016/j.optcom.2015.05.025.

[13] A. Garacia-Zambrana, B. Castillo-Vazquez, and C. Castillo-Vazquez, "Asymptotic error-rate analysis of FSO links using transmit laser selection over gamma-gamma atmospheric turbulence channels with pointing errors," *Optics Express*, vol. 20, no. 3, pp. 2096-2109, Jan. 2012. DOI: 10.1364/OE.20.002096

[14] M. R. Bhatnagar, and Z. Ghssemlooy, "Performance analysis of Gamma–Gamma fading FSO MIMO links with pointing errors," *Journal of Lightwave Technology*, vol. 34, no. 9, pp. 2158-2169, May 2016. DOI: 10.1109/JLT.2016.2526053

[15] I. E. Lee, Z. Ghassemlooy, W. P. Ng, M. A. Khalighi, and S. K. Liaw, "Effects of aperture averaging and beam width on a partially coherent Gaussian beam over free-space optical links with turbulence and pointing errors," Applied Optics, vol. 55, no. 1, pp. 1-9, Feb. 2016. DOI: 10.1364/AO.55.000001

[16] H. Zhang, H. Li, D. Xiao, and S. Ning, "Performance analysis of spatial-diversity reception over combined effects of atmospheric turbulence," *Chinese Journal of Lasers*, vol. 43, no. 4, pp. 0405002, Apr. 2016. DOI:10.3788/CJL201643.0405002

[17] C. Martin and B. Ottersten, "Asymptotic eigenvalue distributions and capacity for MIMO channels under correlated fading," *IEEE Transcations on Wireless Communications*, vol. 3, no. 4, pp. 1350-1359, Aug. 2004. DOI: 10.1109/TWC.2004.830856

[18] H. Moradi, M. Falahpour, H.Refai, and P. Lopresti, "BER analysis of optical wireless signals through lognormal fading channels with perfect CSI," IEEE 17th International Conference on Telecommunications (ICT '10), Doha, pp. 493-497, 2010. DOI: 10.1109/ICTEL.2010.5478870

[19] S. L. Loyka, "Channel capacity of MIMO architecture using the exponential correlation matrix," *IEEE Communications Letter*s, vol. 5, no. 9, pp. 369-371, Oct. 2001. DOI: 10.1109/4234.951380